

THE CLUSTERED NATURE OF STAR FORMATION. PRE-MAIN-SEQUENCE CLUSTERS IN THE STAR-FORMING REGION NGC 602/N90 IN THE SMALL MAGELLANIC CLOUD¹

DIMITRIOS A. GOULIERMIS^{2,3}, STEFAN SCHEMEJA^{4,3}, ANDREW E. DOLPHIN⁵, MARIO GENNARO²,
EMANUELE TOGNELLI^{6,7}, AND PIER GIORGIO PRADA MORONI^{6,7}

Accepted by the Astrophysical Journal January 13, 2012

ABSTRACT

Located at the tip of the wing of the Small Magellanic Cloud (SMC), the star-forming region NGC 602/N90 is characterized by the HII nebular ring N90 and the young cluster of pre-main-sequence (PMS) and early-type main sequence stars NGC 602, located in the central area of the ring. We present a thorough cluster analysis of the stellar sample identified with HST/ACS camera in the region. We show that apart from the central cluster, low-mass PMS stars are congregated in thirteen additional small compact sub-clusters at the periphery of NGC 602, identified in terms of their higher stellar density in respect to the average background density derived from star-counts. We find that the spatial distribution of the PMS stars is bimodal, with an unusually large fraction ($\sim 60\%$) of the total population being clustered, while the remaining is diffusely distributed in the inter-cluster area, covering the whole central part of the region. From the corresponding color-magnitude diagrams (CMDs) we disentangle an age-difference of ~ 2.5 Myr between NGC 602 and the compact sub-clusters which appear younger, on the basis of comparison of the brighter PMS stars with evolutionary models, which we accurately calculated for the metal abundance of the SMC. The diffuse PMS population appears to host stars as old as those in NGC 602. Almost all detected PMS sub-clusters appear to be centrally concentrated. When the complete PMS stellar sample, including both clustered and diffused stars, is considered in our cluster analysis it appears as a single centrally concentrated stellar agglomeration, covering the whole central area of the region. Considering also the hot massive stars of the system, we find evidence that this agglomeration is hierarchically structured. Based on our findings we propose a scenario, according to which the region NGC 602/N90 experiences an active clustered star formation for the last ~ 5 Myr. The central cluster NGC 602 was formed first and rapidly started dissolving into its immediate ambient environment, possibly ejecting also massive stars found away from its center. Star formation continued in sub-clusters of a larger stellar agglomeration, introducing an age-spread of the order of 2.5 Myr among the PMS populations.

Subject headings: Magellanic Clouds – HII regions – Hertzsprung–Russell and C–M diagrams – open clusters and associations: individual (NGC 602) – stars: formation – stars: pre-main-sequence – Methods: statistical

1. INTRODUCTION

Stars are usually born in groups (e.g. Lada & Lada 2003; Stahler & Palla 2005) in a large variety of spatial scales, from small compact clusters to large loose stellar complexes (Efremov & Elmegreen 1998), related to each other in a hierarchical fashion. This hierarchy in the formation of stellar groups is thought to be inherited from the complex hierarchical structure of the interstellar medium (ISM; e.g. Mac Low & Klessen 2004; McKee & Ostriker 2007). The most likely source of this hierarchy is a combination of agglomeration with fragmentation (McLaughlin & Pudritz 1996), self-gravity (Goodman et al. 2009), and turbulence (Elmegreen & Scalo 2004). Stellar structures have hierarchical patterns not only in space, but also in time, suggesting that

their formation takes place faster in the densest regions of a turbulent ISM (Elmegreen 2010).

The Magellanic Clouds (MCs), the nearest galactic companions to the Milky Way, are the best templates of extragalactic star formation due to their closeness to us and their location away from the obscuring Galactic disk. The investigation of star-forming regions in the MCs has been significantly benefitted by the high resolving efficiency over a wide field-of-view provided by the *Hubble Space Telescope* (HST). In particular, recent observations with the *Wide-Field Planetary Camera 2* (WFPC2) and the *Advanced Camera for Surveys* (ACS) on board HST provide a unique opportunity to investigate extragalactic clustered star formation with high spatial resolution and sensitivity in wide-field coverage that corresponds to physical length-scales between ~ 10 and 100 pc.

In our recent study of the stellar clustering behavior of the brightest star-forming region in the Small Magellanic Cloud (SMC), NGC 346/N66, we found that it is hierarchically structured and fragmented into ten individual sub-groups of pre-main sequence (PMS) stars (Schemeja et al. 2009). The interplay between gravoturbulent cloud fragmentation and early dynamical evolution seems to be the main mechanism for building up large star-forming clusters (e.g. Klessen & Burkert 2000; Clark & Bonnell 2005), and our study suggests that this mechanism can best explain our findings in the region NGC 346/N66. Continuing our work on the understanding of clustered star formation in the SMC, we

¹ Based on observations made with the NASA/ESA *Hubble Space Telescope*, obtained at the Space Telescope Science Institute, which is operated by the Association of Universities for Research in Astronomy, Inc. under NASA contract NAS 5-26555.

² Max Planck Institute for Astronomy, Königstuhl 17, 69117 Heidelberg, Germany

³ Zentrum für Astronomie der Universität Heidelberg, Institut für Theoretische Astrophysik, Albert-Ueberle-Str. 2, 69120 Heidelberg, Germany

⁴ Zentrum für Astronomie der Universität Heidelberg, Astronomisches Rechen-Institut, Mönchhofstr. 12-14, 69120 Heidelberg, Germany

⁵ Raytheon Company, PO Box 11337, Tucson, AZ 85734, USA

⁶ Dipartimento di Fisica “Enrico Fermi”, Università di Pisa, largo Pontecorvo 3, Pisa I-56127, Italy

⁷ INFN-Sezione di Pisa, largo Pontecorvo 3, Pisa I-56127, Italy

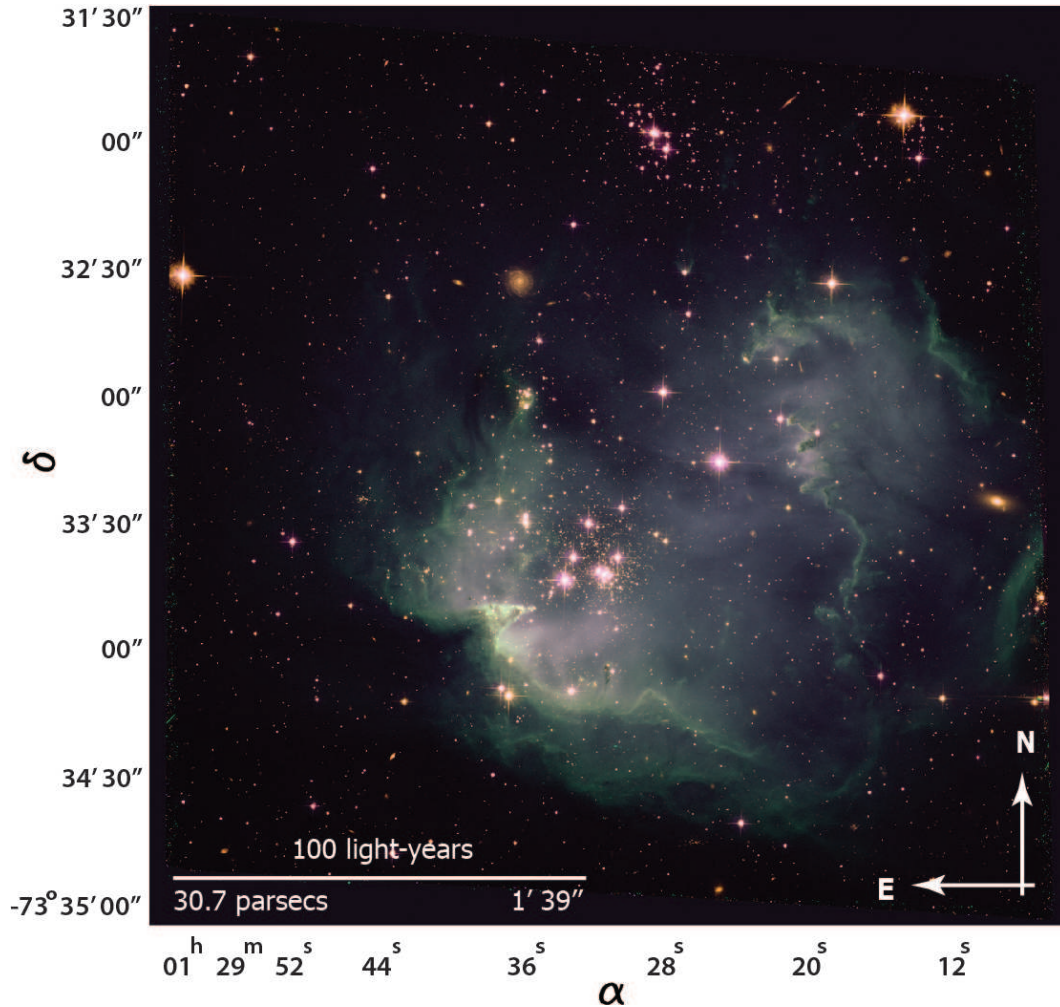


FIG. 1.— Color composite image of exposures made by ACS/WFC in two broadband filters, F555W (V) and F814W (I), and one narrowband filter, F658N ($H\alpha$ & $[NII]$) of the region NGC 602/N90. The young cluster NGC 602 lies inside the ring-shaped nebula N90, the edges of which are eroded by the radiation of the hot young stars, producing the spectacular bubble. Ridges of dust and gaseous filaments are seen towards the northwest and the southeast. Dusty pillars point towards the center giving signs of the eroding effect by the central hot blue stars. Candidate YSOs found along the surrounding dust ridges give evidence that star formation has possibly started at the center of the region and advanced outward. In this study PMS stars are found to be distributed in a diffuse manner centered on NGC 602, as well as concentrated in younger compact peripheral sub-clusters along the inner rim of the bubble, providing support to the above suggestion.

investigate here another star-forming region, NGC 602/N90 (Fig. 1).

This region, located in the wing of the SMC, seems to represent a different, less complex, mode of star formation than that of NGC 346/N66 (see also Gouliermis et al. 2007, 2008). The emission nebula LHA 115-N90 (Henize 1956), or in short N90⁸, is a ring-shaped HII region with the bright young cluster NGC 602 (Westerlund 1964; Hodge 1985) located in its cavity. Being quite isolated and remote from the main body of the SMC this rather small star-forming region (with a physical size of ~ 60 pc) has attracted interest in various investigations due to its brightness. Its stellar population is known to comprise massive hot stars younger than 15 Myr (e.g. Battinelli & Demers 1992; Massey et al. 2000), with the eleven brightest stars being early-type dwarfs with spectral types between O6 and B5 (Hutchings et al. 1991).

The metallicity and dust-to-gas ratio of NGC 602/N90 does not seem to differ from typical values for the SMC, being $[Fe/H] \simeq -0.65$ (e.g. Rolleston et al. 1999; Lee et al. 2005), and $\sim 1/30$ of that in the Milky Way (Stanimirovic et al. 2000) respectively. The region is presumed to have been

formed in a relatively isolated and diffuse environment by a star formation event that was produced by compression and turbulence associated with HI shell interactions, started at ~ 7 Myr ago, leading to the formation of stars ~ 3 Myr later, i.e., 4 Myr ago (Nigra et al. 2008). However, observations with the *Spitzer Space Telescope* (STT) show that the region still hosts ongoing star formation demonstrated by a number of candidate massive Young Stellar Objects (YSOs; Carlson et al. 2007; Gouliermis et al. 2007; Carlson et al. 2011). Moreover, imaging with HST/ACS of the region revealed a plethora of candidate PMS stars with masses reaching the sub-solar regime (Carlson et al. 2007; Schmalzl et al. 2008; Cignoni et al. 2009).

Preliminary studies of the spatial distribution of these stars show that they are not homogeneously distributed across the region, but they are grouped in discrete compact concentrations. Some of those compact sub-clusters at the periphery of the bubble of N90 are found to coincide with candidate YSOs (Gouliermis et al. 2007; Carlson et al. 2011), suggesting that they are probably still embedded. In this paper we perform a thorough cluster analysis on the rich PMS population unveiled by HST/ACS in the bright SMC star-forming region NGC 602/N90 (Fig. 1). The aim is to analyze the stellar clus-

⁸ N90 is also known as DEM S 166 (Davies et al. 1976)

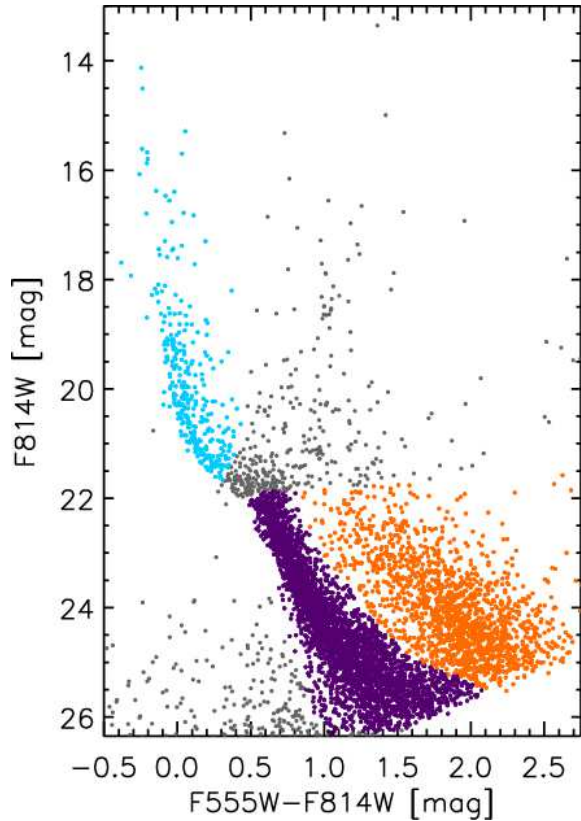


FIG. 2.— F555W–F814W, F814W CMD of all stars found in the region NGC 602/N90 with ACS/WFC imaging. The members of the three dominant stellar types, i.e. UMS, LMS and PMS stars (see § 3.1), are plotted with light-blue, purple and orange colors respectively.

tering behavior of the region and to compare our results to current scenarios of star formation in order to achieve a more comprehensive understanding of clustered star formation in the isolated environment of the SMC wing.

We make use of our deep ACS photometry (Schmalzl et al. 2008), and we apply the star-counts algorithm to isolate local stellar density enhancements from the underlying density background and to identify all PMS clusters in the region. The dataset is presented in § 2. The stellar content of the region and the thorough selection of the PMS population are described in § 3.1. The detection of individual young stellar clusters in the region with the application of *star-counts*, and the extraction of their structural parameters is performed in § 4, where also the stellar content of the individual sub-clusters and their surrounding area is investigated. The clustering behavior of the young stellar content of the region is further quantified with the application of the *minimum spanning tree* method, which takes place in § 5. In § 6 we discuss our results in terms of the star clusters formation process as it is revealed from our analysis, and propose a scenario that may sufficiently explain this process in the region. We give our concluding remarks in § 7.

2. OBSERVATIONS AND PHOTOMETRY

The observations used in this study are taken with the Wide-Field Channel (WFC) of ACS within the HST GO Program 10248 (PI: A. Nota). The HST images of one pointing, centered on the young cluster NGC 602, observed in the filters F555W ($\equiv V$) and F814W ($\equiv I$), were retrieved from the

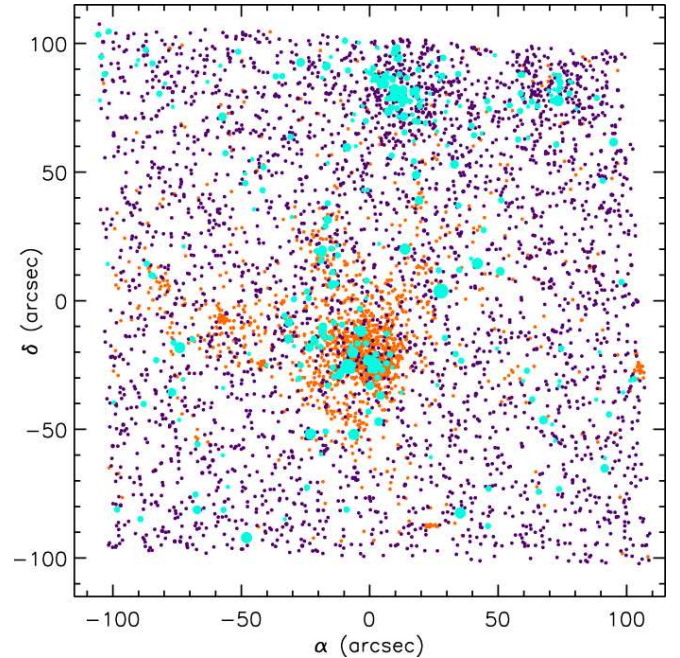


FIG. 3.— The stellar chart of stars identified with our photometry in the observed WFC pointing. Stars are color-coded according to their types, as derived from their CMD positions; light-blue for UMS, purple for LMS, and orange for PMS stars (see text in § 3.2). Larger blue symbols correspond to brighter UMS stars. Turn-off stars are not plotted. The map is centered according to the observed WFC pointing (J2000 22:21:53.55 –73:33:17.14).

HST Data Archive⁹. These images cover an area of about $3.4' \times 3.5'$ ($\sim 58 \text{ pc} \times 58 \text{ pc}$ at the distance of the SMC). The reduction and photometry of the data is discussed in detail in Schmalzl et al. (2008), within our investigation of the Initial Mass Function in the region. Photometry was performed using the ACS module of the package DOLPHOT, an adaptation of the photometry package HSTphot (Dolphin 2000), and after eliminating bad detections more than 5 626 stars down to $m_{555} \simeq 26.5$ mag were included in the photometric catalog, with a completeness of $\gtrsim 50\%$ down to $m_{555} \approx 25$ mag. The corresponding *VI*-equivalent color-magnitude diagram (CMD) is shown in Fig. 2.

3. STELLAR CONTENT OF THE REGION

3.1. General description of the stellar content

Previous studies in the region NGC 602/N90 show that it comprises three individual dominant stellar clusters and a variety of stellar types (Carlson et al. 2007; Gouliermis et al. 2007; Schmalzl et al. 2008; Cignoni et al. 2009; Carlson et al. 2011). In particular, apart from the young cluster NGC 602 located almost at the center of the ring-shaped nebula, the observed ACS field covers two more evolved open clusters north of the HII ring (see also Fig. 3). We select the different stellar types in the region by first dividing the main-sequence (MS) stars of our photometric catalog into Upper MS (UMS) and Low MS (LMS) stars in terms of their colors and magnitudes in the CMD of Fig. 2. The UMS stars are considered to cover the part of the CMD defined by the conditions:

$$\begin{aligned} m_{555} - m_{814} &\leq 0.45 \quad \text{and} \\ m_{555} - m_{814} &\leq -0.2 m_{814} + 4.65. \end{aligned}$$

⁹ The HST Data Archive is accessible from MAST at <http://archive.stsci.edu/hst/>, and ESO at <http://archive.eso.org/cms/hubble-space-telescope-data>.

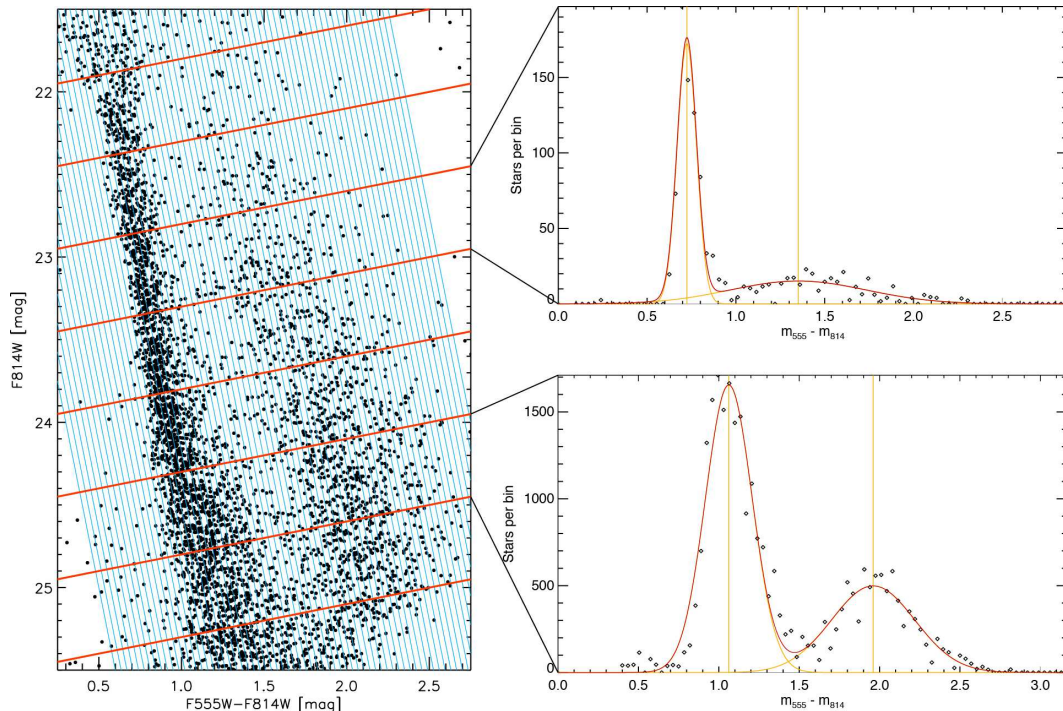


FIG. 4.— Schematic of the selection of the low-mass PMS stars through their number distributions along cross-sections of the faint part of the observed CMD. Two examples of these distributions are given, where it can be seen that MS and PMS stars are well separated by their individual components (peaks) in the distribution. Even at brighter magnitudes, where the MS population is most prominent (top distribution), the PMS stars can be identified from their second, wider, red peak. At fainter magnitudes (bottom distribution) the distinction between MS and PMS stars is even more obvious. The vertical scales in the right hand plot are not the same.

This selection is marked in Fig. 2 by plotting the UMS stars with a light-blue color. The LMS (as well as the low-mass PMS) stars are selected to have magnitudes $m_{814} \geq 22$. The remaining part of the CMD is considered to be populated mostly by the turn-off and evolved red stellar populations. Stars in this part are plotted with grey symbols in Fig. 2.

While UMS stars are the most bright members of all three dominant stellar clusters in the region, the LMS stars characterize *only* the more evolved northern open clusters and the general background SMC field. This can be seen in the stellar map of the region, shown in Fig. 3, where stars are again color-coded according to their types. There are no low-mass PMS stars in the northern clusters, as they can only be found in the central cluster NGC 602 and its immediate surroundings. This is discussed in more detail in the following section. Concerning the covered background field of the SMC, it comprises the most evolved observed populations (e.g., Sabbi et al. 2009), which, apart from the LMS, include the turn-off and the sparse sub- and red-giant branches. There is an apparent overlap between the MS turn-off and the PMS-MS transition (turn-on), and therefore these stars will not be considered in the analysis of the following section to avoid confusion by their appearance in the CMD. This exclusion does not affect the subsequent selection of low-mass PMS stars, because they are selected to be fainter than the turn-off magnitude.

3.2. Low-mass pre-main-sequence stars

In the CMD of Fig. 2 the low-mass PMS stars can be distinguished from the LMS stars, located at the blue part of the CMD. Indeed, in previous investigations faint PMS stars in the region are selected by their mere location to the red part of the CMD. However, the positive identification of the true faint PMS stars, especially those closer to the MS, requires

an accurate quantitative approach in order to eliminate any contamination by reddened or binary LMS stars. We perform such an analysis by counting the number of stars as a function of their $(m_{555} - m_{814})$ colors along a series of CMD cross-sections perpendicular to the PMS locus. This process is demonstrated in Fig. 4, where the faint CMD of the region is shown (left panel) with the cross-sections indicated by the red lines. The cross-sections are selected to have a width of $\Delta m_{F814W} \sim 0.5$ mag. For the construction of the corresponding stellar distribution along each cross-section, stars are binned in strips perpendicular to the cross-sections and thus approximately parallel to the MS. These strips, which are also almost parallel to typical PMS isochrones, are indicated in Fig. 4 by the blue lines. This method was originally used for the identification of PMS stars in *VI* CMDs of Galactic star-forming regions (see, e.g., Sherry, Walter, & Wolk 2004). Its recent application to WFC2 photometric data of four star-forming regions in the Large Magellanic Cloud showed that it can be very efficient in distinguishing the faint PMS from the MS, even in CMDs with higher confusion than the one shown here (Gouliermis et al. 2011). Two examples of the constructed stellar distributions along the CMD cross-sections, i.e., one on a brighter (top) and another on a fainter cross-section (bottom), are shown in Fig. 4 (right panel). The numbers of stars per bin shown in these distributions, as well as for all constructed stellar distributions, are corrected for photometric incompleteness according to our completeness measurements, performed in Schmalzl et al. (2008).

From Fig. 4 it can be seen that the distribution of stars along the cross-sections through the CMD can be well represented by the sum of two distributions; one for the LMS and one for the PMS stars. We fit the number of stars per bin of the constructed distributions to a double Gaussian function as shown in the examples of Fig. 4, where the total fit is plotted by a red

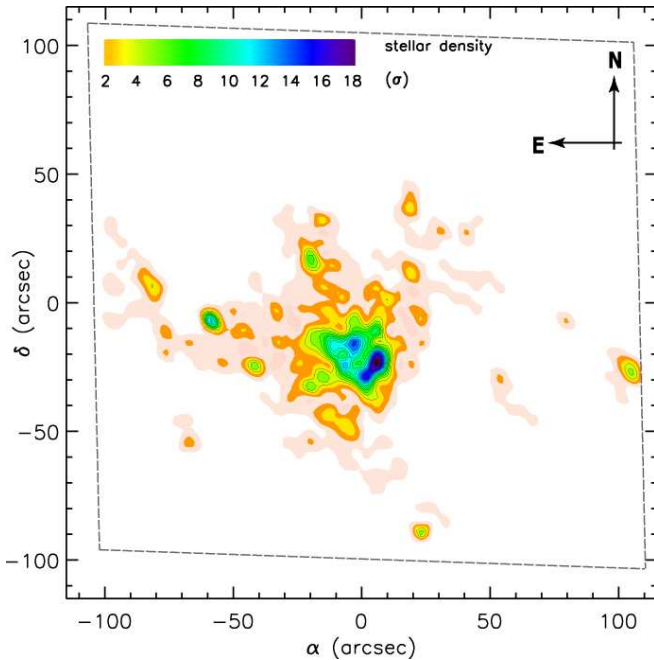


FIG. 5.— Stellar density contour map of the low-mass PMS stars in the observed region. Isodensity contours are drawn according to their levels defined in σ above the average density, as indicated by the color bar at the top. This map shows that apart from the main young cluster NGC 602, there are distinct compact sub-clusters of PMS stars located at the inner part and at the periphery of the HII ring. The observed ACS field-of-view is indicated by the grey dashed lines. Cluster 5 (see also § 4.2 and Fig. 6) is at the edge of this field.

line, while the individual components by orange lines. The functional form of our fit is

$$y = \sum_{i=1}^2 N_i e^{-0.5((x-\mu_i)/\sigma_i)^2}, \quad (1)$$

where the first term describes the distribution of the LMS and the second that of the PMS stars. We use a least-squares multiple Gaussian fit performed by the interactive IDL routine XGAUSSFIT (by Don Lindler) to solve for six parameters, N_i , μ_i , and σ_i , where $i = 1$ is for the LMS and $i = 2$ for the PMS stars. In this fitting process, which is performed for the stellar distributions along each of the selected cross-sections, μ_i is the color $m_{555} - m_{814}$ of the peak of the distribution, indicated with yellow vertical lines in the examples of Fig. 4, N_i represents the number of stars that correspond to the peak of the distribution, and σ_i defines the width of the Gaussian. The full width at half maximum (FWHM) of each Gaussian is then $2\sigma_i \sqrt{2 \ln(2)}$ for each cross-section. The minimum between the two Gaussian components for every cross-section defines the limits between MS and PMS stars on the CMD. We specified, thus, the region of the PMS stars on the CMD by a line defined by the minima where the two Gaussians overlap. Based on this method we determine the low-mass PMS members in the region. They are color-coded in orange in the CMD of Fig. 2 and in the stellar map of Fig. 3.

4. SPATIAL DISTRIBUTION OF PMS STARS IN NGC 602/N90

The stellar chart of all three dominant stellar types, i.e., UMS, LMS and PMS stars, selected as described above, is shown in Fig. 3. There is a definite spatial distinction among different stellar types, with most of the LMS and UMS stars being concentrated in the northern open clusters, while the vast majority of the low-mass PMS, along with the hottest

(OB-type) stars in the region as we discuss later, are located at the vicinity of the young star cluster NGC 602. This is in line with the findings of previous studies, according to which NGC 602 is at an earlier stage of its stellar evolution than the northern clusters (e.g., Schmalzl et al. 2008). The fact that the brightest UMS stars are indeed located in the vicinity of NGC 602 (Hutchings et al. 1991) signifies further its youth. In the chart of Fig. 3 it can also be seen that low-mass PMS stars seem not to be centrally concentrated. There is a clear ‘diffused’ distribution of these stars, almost surrounding NGC 602, as well as distinct concentrations located within the vicinity of, but still away from, the central cluster. We develop an automated algorithm for the detection of stellar density enhancements and their distinction from the background density, based on classical star-counts (see, e.g., Kontizas et al. 1994). The star-count method is found to perform comparably or usually better than other methods such as *nearest neighbor* density or *minimum spanning tree* separation (Schmeja 2011). We evaluate the spatial distribution of low-mass PMS stars in the region quantitatively and we assess their clustering behavior by identifying several ‘peripheral’ small compact PMS sub-clusters in the region as statistically important density enhancements. We describe this analysis in the following section.

4.1. Analysis of the surface density of PMS stars

In order to identify concentrations of PMS stars in the observed region, we construct the stellar density map by performing star-counts in a grid of quadrilateral elements. We bin the low-mass PMS stars according to their positions in a grid of 50×50 elements, corresponding to a scale of about $4''$, i.e., ~ 1 pc per grid element. This grid element size is empirically chosen after applying several tests to grids with elements of different sizes. Smaller sizes of elements in the star-count grid allow the appearance of noise in the density maps as a large number of small peaks, which correspond to density fluctuations rather than true stellar clusterings. On the other hand, grids with larger elements would ‘smear out’ individual density peaks by grouping distinct compact clusters into larger objects, and thus would not allow us to identify the fine-structure in the surface stellar density of the region. The star-counts grid was aligned according to the stellar chart of Fig. 3, i.e., it is oriented so that its x- and y-axes coincide with the R.A. and Decl. respectively. The grid is designed so that the top-left and bottom-right corners of the star-counts map to coincide with those of the observed ACS field-of-view. The derived stellar density map is shown in Fig. 5. In this figure isopleths are drawn in steps equal to the standard deviation, σ , of the average density. The lowest contour corresponds to the 1σ density level, indicated with faint pink color in Fig. 5. From this map one can deduce that the large majority of low-mass PMS stars is indeed concentrated in the area of the central young cluster NGC 602, and that the cluster itself is *not* symmetric.

In addition, the density map of Fig. 5 shows that apart from the central cluster, there are several ‘clumps’ of PMS stars, which can be seen within the boundaries of the lowest density isopleth. These are small in size compact sub-clusters of PMS stars, which stand out due to their high stellar density. Outside these clusters a diffuse PMS stellar distribution fills the space between them. Both these features in the surface density of low-mass PMS stars reveal their clustering behavior in the region NGC 602/N90. This behavior can be described as most of the PMS stars being centrally concentrated in the cluster

TABLE 1
BASIC CHARACTERISTICS OF THE DETECTED PMS STAR CLUSTERS.

Cluster no.	R.A. (deg J2000)	Decl.	r_{equiv} (pc)	$m_{555,\text{tot}}$ (mag)	N_*	$N_{*,\text{cc}}$	ϱ stars pc^{-3}	\mathcal{Q}^a	$\sigma_{\mathcal{Q}}$	YSOs ^b
1	22.383888	-73.560593	6.65	13.018	1028	21298	23.1	0.80	0.02	Y251
2	22.397900	-73.550407	2.51	17.202	61	1112	22.4	0.87	0.05	Y327
3	22.389244	-73.568047	2.02	16.194	44	681	26.3	0.70	0.05	Y171
4	22.436224	-73.556877	1.45	20.830	43	1390	145.2	0.88	0.05	Y326
5	22.277424	-73.563522	1.35	18.636	31	132	17.1	0.79	0.05	Y096
6	22.421598	-73.561874	1.20	19.226	25	425	78.3	0.78	0.07	
7	22.459705	-73.552544	1.39	19.246	25	936	111.0	0.54	0.08	
8	22.360380	-73.544899	1.05	17.400	15	395	108.7	0.69	0.09	
9	22.359076	-73.579903	0.91	23.704	14	384	162.3	0.77	0.09	Y090
10	22.425650	-73.557953	1.06	22.779	12	532	142.3	0.85	0.09	
11	22.393993	-73.546204	0.84	17.603	11	534	286.9	0.72	0.10	
12	22.412523	-73.555962	0.87	20.661	10	322	155.7	0.62	0.12	Y312
13	22.360632	-73.552063	1.07	23.354	9	267	69.4	0.94	0.12	
14	22.356310	-73.557083	0.97	22.750	8	128	44.7	0.91	0.12	

NOTE. — For explanations on the columns see § 4.2. The total brightness $m_{555,\text{tot}}$ of each cluster is the cumulative brightness of all stars identified within the boundaries of the cluster. N_* is the total number of observed stars per cluster, and $N_{*,\text{cc}}$ is the same number with completeness corrections applied. Sub-cluster 1 corresponds to the main cluster NGC 602.

^aThe derivation of the parameter \mathcal{Q} and typical uncertainties $\sigma_{\mathcal{Q}}$ in its measurement are described in § 5.

^bYSO candidates IDs from Carlson et al. (2011).

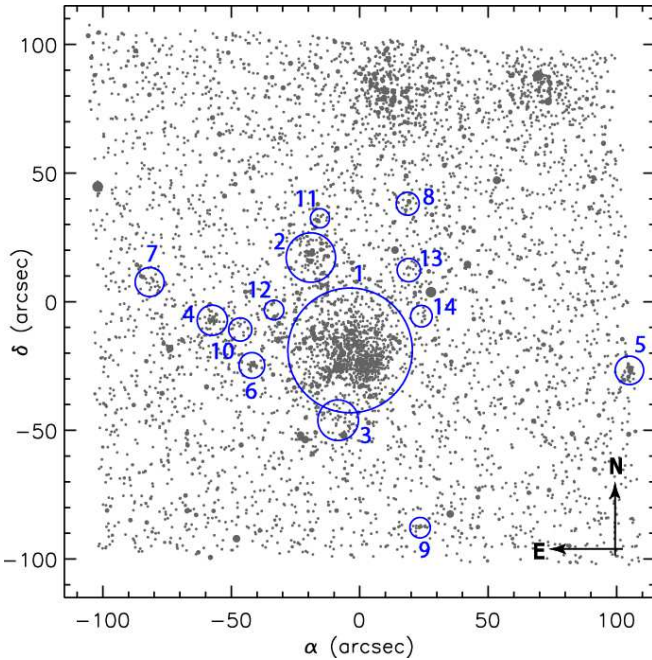


FIG. 6.— Positions of the PMS clusters identified in the region with star counts, plotted on the full stellar map. The clusters are defined by circular annuli with radii equal to their equivalent radii, as given in Table 1. They are also annotated by their incremental number, as given in the same table. All sub-clusters, except 5 and 9, seem to be contained in a larger aggregate of stars defined by the average PMS stellar density (Fig. 5). This indicates a possible evolutionary and dynamical connection among them.

NGC 602 and in small compact peripheral sub-clusters, which in turn seem to be surrounded by a general diffuse distribution of the same type of stars.

4.2. Identification of PMS Sub-Clusters

According to our methodology, we consider any stellar concentration revealed in the map of Fig. 5 by the isopleths that correspond to stellar density of at least 3σ above the background (indicated by the yellow-colored contours) as being *statistically important*, and thus as a candidate star cluster. As discussed above, these clusters are not completely isolated

from each other, but they appear to be members of a larger concentration of PMS stars. We define the boundaries of each of these clusters by their limits according to the 2σ isopleth in the density map, and we measure the corresponding ‘equivalent’ radius as

$$r_{\text{equiv}} = \sqrt{\frac{A}{\pi}}, \quad (2)$$

where A is the surface enclosed by the threshold isopleth, assuming circular symmetry in their shapes. We select the stellar members of each cluster from the original photometric catalog of all stars (not PMS stars alone), by the positions of the stars as they are confined by the 2σ isopleth as well. With this method we identified 14 distinct PMS sub-clusters, NGC 602 included.

The positions of the identified sub-clusters are annotated in the stellar map of Fig. 6, and their characteristics are given in Table 1. The identity numbers of the sub-clusters are given in Col. 1 of the table. Their coordinates, given in Cols. 2 and 3, are derived from their baricenters, i.e., the average positions of all their stellar members. Their equivalent radii and total brightness (not corrected for incompleteness) are given in Cols. 4 and 5 respectively. The original total numbers of stars (of all types) in each sub-cluster are shown in Col. 6 of Table 1, and in Col. 7 these numbers are corrected for incompleteness according to our completeness measurements in Schmalzl et al. (2008). Naturally, since we are limited by the detection efficiency of our photometry, these corrections are limited to $\sim 50\%$ completeness and therefore they do not reflect the true total stellar numbers of each sub-cluster. They can be used though for an estimate of the volume stellar density of the clusters, which reflects their compactness. We give this estimate for every sub-cluster in Col. 8 of the table. The \mathcal{Q} parameter, which permits us to quantify the structure of a cluster and to distinguish between centrally concentrated and hierarchical clusters and typical uncertainties, $\sigma_{\mathcal{Q}}$, in its determination (see § 5) are given in Cols. 9 and 10 respectively. Finally, the YSO candidates from the catalog of Carlson et al. (2011), which are found to match the positions of our sub-clusters (see § 4.3) are given in Col. 11 of Table 1. It should be noted that among the identified sub-clusters, cluster 5 be-

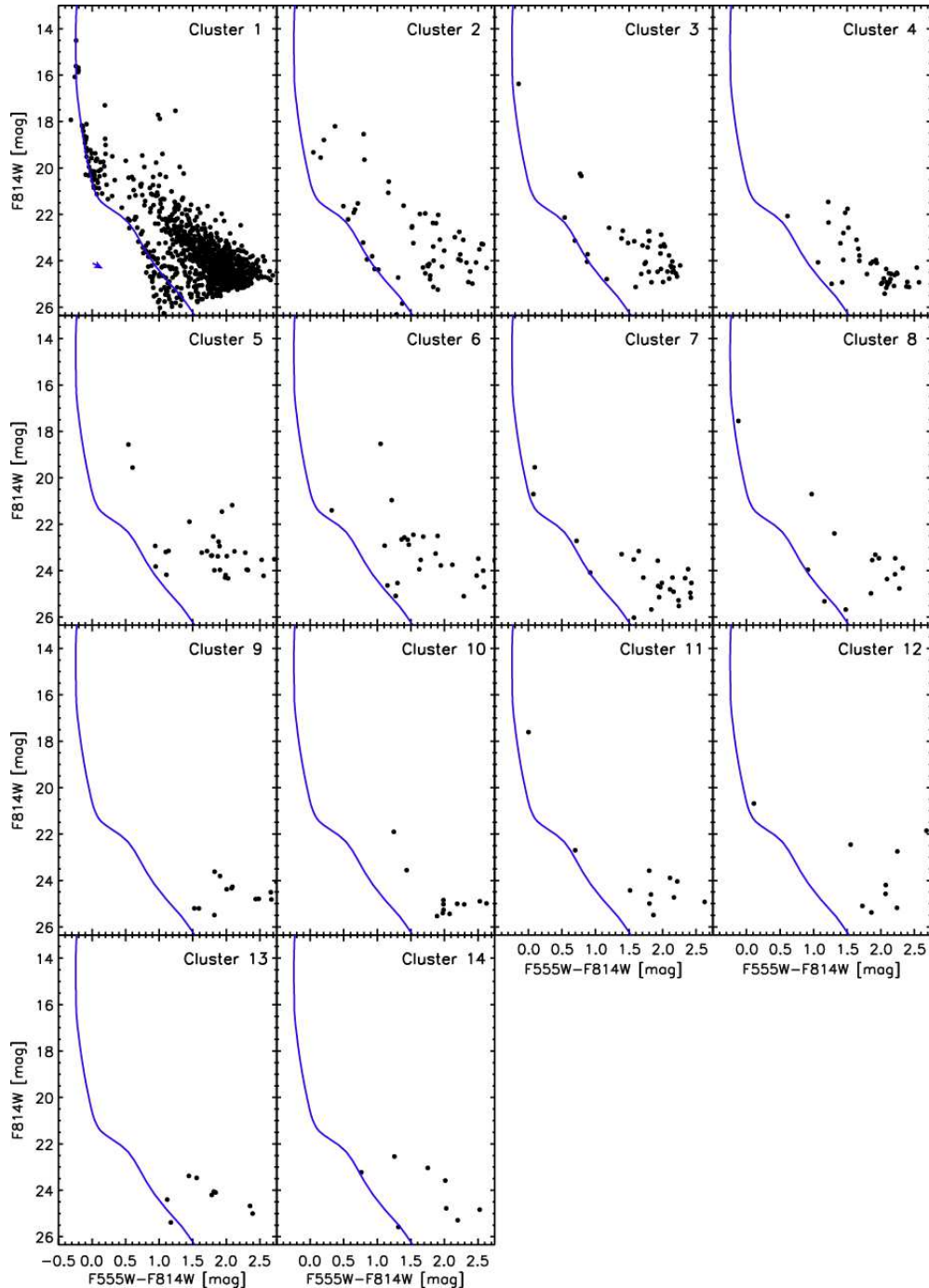


FIG. 7.— F555W–F814W, F814W CMDs of the PMS sub-clusters found in the region NGC 602/N90. The ZAMS from the Padua set of models (Girardi et al. 2002) for the metallicity of the SMC ($Z = 0.003$), is plotted in blue for guidance. It is corrected for a distance modulus of $m - M \simeq 18.95$ mag, and an extinction of $A_V \simeq 0.3$ mag (Schmalzl et al. 2008) represented by the reddening vector plotted at the lower left quadrant of Cluster 1 CMD.

ing located on the edge of the observed field-of-view, extends somewhat out of this field as can be seen in IRAC images of the region (see, e.g., Carlson et al. 2011). Therefore, its derived parameters should be considered as the lower limits.

4.3. Stellar content of the identified clusters

The individual CMDs of the detected PMS clusters are shown in Fig. 7. These CMDs are constructed from all stars included within the boundaries of the sub-clusters, as described above, their numbers being given in Col. 6 of Table 1. As shown in this figure, these numbers for about half of the sub-clusters are very low, not enough to extract signif-

icant information. We show the CMDs with an overlaid *Zero Age Main Sequence* (ZAMS) for guidance. The CMDs of the less populous sub-clusters, with identification numbers 9 and higher, are shown in the third and forth panels of Fig. 7. It is interesting that while some sub-clusters host stars in a wide range of magnitudes, other and in particular the less populous host mostly only faint PMS stars, down to our detection limit. It is also worth noting that some of the detected sub-clusters appear bright in mid-IR wavelengths as seen with the *Spitzer Space Telescope* (STT). In particular, we matched the positions of our sub-clusters with those of the candidate YSOs population in the region derived by Carlson et al. (2011), and

we found that seven of the sub-clusters coincide with one YSO each; we provide the YSO identities in Col. 11 of Table 1. It should be noted that YSO candidate Y251 does not quite coincide with the cluster NGC 602, but is on the eastern edge within its boundaries. The other YSO candidates coincide with the whole extent of their matching star clusters, which are very small. This is a natural result of the low resolving power of SST.

Low-mass PMS stars in star-forming regions of the MCs are widely spread in the red-faint part of their optical CMDs (see, e.g., Cignoni et al. 2009; Vallenari et al. 2010; Gouliermis et al. 2011, for recent results). As a consequence, according to PMS evolutionary models the CMD positions of these stars imply a broad coverage in ages, which may be indicative of an age-spread. However, previous investigations have shown that the broadening of the loci of faint PMS stars in the optical CMD does not necessarily provide proof of an age-spread, since it may well be the result of biases introduced by observational constraints, i.e., photometric accuracy and confusion. The CMD positions of these stars depend also on their physical characteristics, such as variability, binarity and circumstellar extinction (see, e.g., Da Rio, et al. 2010 and Jeffries 2011, for detailed discussions), making the determination of their ages from isochrone fitting quite challenging. Under these circumstances, it is not possible to extract absolute ages of such stars, unless thorough modeling of their positions is being applied.

In star-forming regions differential reddening may also be considered as an important factor for the broadening of faint PMS stars in the observed CMDs, but in NGC 602/N90, according to our measurement of $\langle A_V \rangle \simeq 0.2$ with a variance of $\simeq 0.07$ (Schmalzl et al. 2008), interstellar reddening cannot be accounted for the observed CMD-broadening. A reddening vector corresponding to $A_V \simeq 0.3$ is shown in the top-left corner of the first CMD of Fig. 7 to demonstrate the small effect of variable optical extinction to the observed CMD positions of the PMS stars. As we discuss later, some of the identified sub-clusters show bright IR emission, coinciding with known YSOs (Carlson et al. 2011), indicating that possibly they are still embedded in their natal clumps. Considering the above discussion about the CMD-broadening of PMS stars in all detected sub-clusters, we use here a set of PMS evolutionary models not to determine their ages from their PMS populations, but to define an upper limit for these ages on a comparative basis. It is worth noting that the stellar numbers included in each sub-cluster are too few to provide a solid age determination, except of very few cases.

We used the most recent Pisa PMS models which rely on the state-of-the-art of input physics and are available for a wide range of Z , Y , α , mass, and age values¹⁰ (see Tognelli et al. 2011, for a detailed description). These models have been computed with an updated version of the *Frascati Raphson Newton Evolutionary Code* (FRANEC), a well-tested Henyey evolutionary code (Degl’Innocenti et al. 2008), for the canonical metal abundance of the SMC, namely $[\text{Fe}/\text{H}] = -0.65$ ($Z = 0.003$ and $Y = 0.254$). The Pisa PMS database provides models with three different values of the mixing-length parameter α , namely 1.2, 1.68 (solar calibrated) and 1.9. In this study we use tracks with $\alpha = 1.2$, which provide the best fit of the data in agreement with other indications from binary systems (Simon et al. 2000; Steffen et al. 2001; Stassun et al.

2004; Gennaro et al. 2011) and Li-depletion (Ventura et al. 1998; D’Antona & Montalbán 2003; Tognelli et al. 2001b) studies. We transformed tracks and isochrones from the theoretical plane into the ACS/WFC VEGAmag photometric system for a direct comparison with our photometry by using the synthetic spectra provided by Brott & Hauschildt (2005) for $T_{\text{eff}} \leq 10000$ K and by Castelli & Kurucz (2003) for $T_{\text{eff}} > 10000$ K.

In Fig. 8 we show the CMDs of the eight most populous sub-clusters in our sample, i.e., clusters that include enough stars for a meaningful comparison with isochrones. The contribution of the field stellar population is removed from the CMDs using a statistical subtraction technique based on the Monte Carlo method after selecting the least populated area of the region as the most representative of the field population (see Schmalzl et al. 2008, for a detailed description). Indeed, a comparison between the CMDs of Fig. 8 with those of Fig. 7 for the same clusters show that the LMS, as well as the turn-off and sub-giants are essentially eliminated after the decontamination of the field. This subtraction is in particular interesting for the most populous cluster, i.e., NGC 602 (cluster 1). In Fig. 8 FRANEC PMS isochrones for ages 0.5, 1, 1.5, 2.5 and 5 Myr are overlaid with different colors. From these isochrones one can deduce that all sub-clusters are quite young, with ages $\lesssim 5$ Myr, considering the broadening of the PMS stars and the fact that the 5 Myr model is quite away to the blue from the observed CMD-location of the faint PMS populations. Nevertheless, from the inspection of the individual CMDs one can also conclude that not all sub-clusters appear to have the same age, with clusters 2, 5 and 6 appearing to be as young as 1 Myr.

While the observed broadening of the CMD-positions of faint PMS stars with $m_{F814} \gtrsim 21$ does not allow us an accurate age determination for the sub-clusters, the CMD-locations of the brighter PMS stars are less affected by photometric uncertainties or other sources of luminosity spread, such as variability, unresolved binarity or circumstellar extinction and therefore they are more successfully fitted by the appropriate isochrones. Moreover, considering that these stars are located at the turn-on in the CMD, where the isochrones of different ages are more distinct to each other, these stars are more accurate chronometers of their hosting clusters. We consider, thus, the bright PMS stars of the CMDs shown in Fig. 8 with magnitudes $18 \lesssim m_{814} \lesssim 21$ and colors $0.0 \lesssim m_{555} - m_{814} \lesssim 1.5$. A comparison of the CMD-locations of these stars in respect to the overlaid isochrones between different sub-clusters shows that indeed it seems that they do have different ages.

In particular, the bright PMS stars in both the most well-populated sub-clusters 1 and 2 seem to fit very well the PMS-MS transit phase, i.e., the turn-on, but for different ages. Specifically, taking the isochrones fit of these stars at ‘face value’ it seems that sub-cluster 1 (NGC 602) is older than sub-cluster 2, since the turn-on of sub-cluster 1 fits better to an age of $\lesssim 5$ Myr, while that of sub-cluster 2 to an age of $\lesssim 2.5$ Myr. As far as the rest of the sub-clusters are concerned, the very few bright PMS stars in them do not allow definite age distinctions from the others. However, the positions of these stars, where are apparent, show a trend to younger ages and in particular around 2.5 Myr. This result is in agreement with that of Cignoni et al. (2009), who found that star formation in the region NGC 602/N90 in the recent 10 Myr has been quite high, reaching a peak in the last 2.5 Myr. Nevertheless, it can only serve as an indication of a possible age difference

¹⁰ The Database is available at <http://astro.df.unipi.it/stellar-models/>

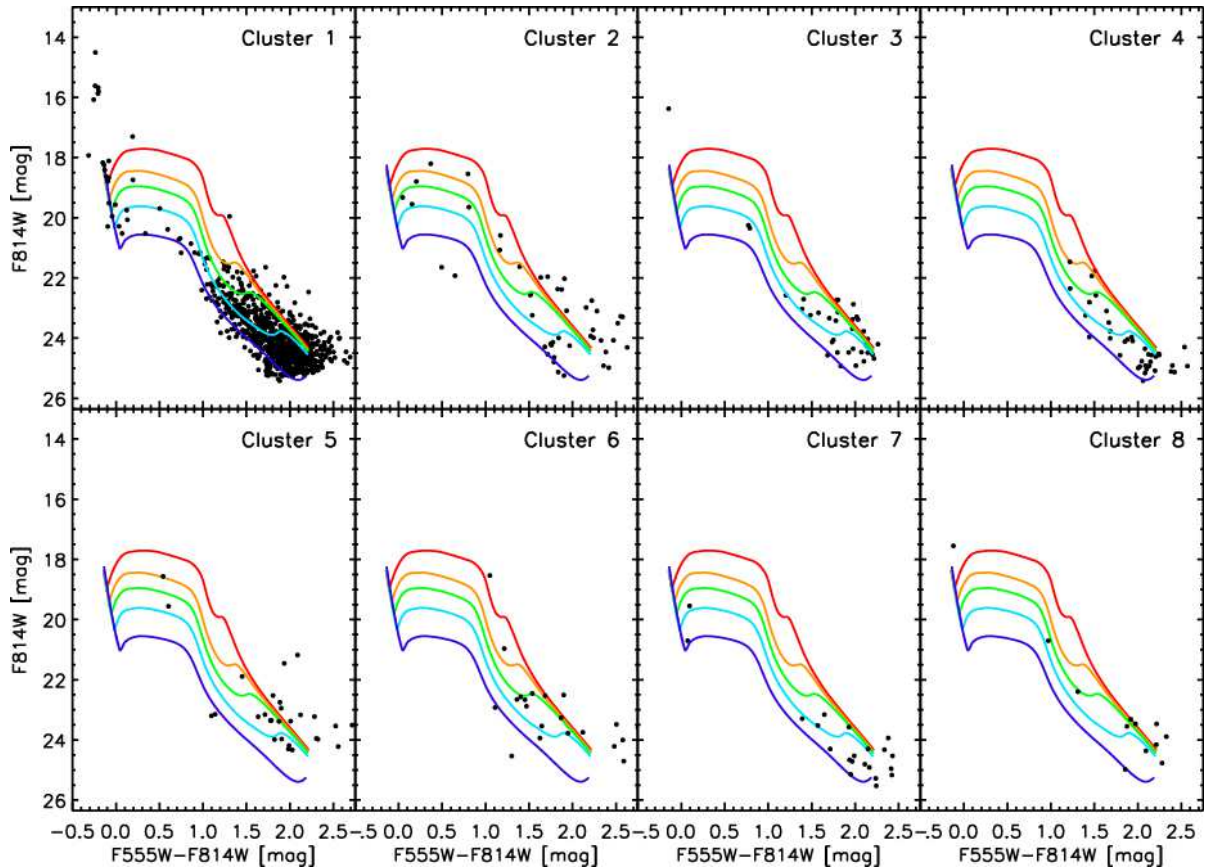


FIG. 8.— F555W–F814W, F814W CMDs of the eight most populous PMS sub-clusters in the region NGC 602/N90. PMS isochrone models calculated with FRANEC (Tognelli et al. 2011) are overlaid in different colors to demonstrate that while an absolute age for the sub-clusters is not possible to be determined, an upper limit for this age can be well established. The models correspond to ages of 0.5 (red), 1.0 (orange), 1.5 (green), 2.5 (light blue), and 5.0 (blue) Myr. They are corrected for distance and extinction.

between the sub-clusters, and not as a direct proof.

No additional information can be provided by the faint PMS populations of the sub-clusters. From these populations, and the comparison of their CMD positions with the PMS isochrones we see that in some sub-clusters (e.g., sub-clusters 2, 5, and 6) faint PMS stars are extremely red, located outside the coverage of the models, while in others (e.g., sub-clusters 3 and 4) they appear well distributed among the selected models. This difference may reflect age differences among the clusters, in the sense that redder stars are younger. Higher extinction in the most embedded clusters can also shift stars redward on the CMD, making them appear younger.

Concerning the candidate YSOs identified in the sub-clusters (Carlson et al. 2011, see also Table 1), as mentioned earlier there is one candidate included within the outer boundaries of sub-cluster 1, but not quite coinciding with the main part of the cluster. On the other hand, each of sub-clusters 2, 3, 4 and 5 does coincide at its complete extent with IR-bright candidate massive YSOs. Previous independent studies that combine observations from both HST and SST note that objects that appear as massive YSOs in mid-IR bands can be resolved into multiple PMS sources in the optical (Gouliermis et al. 2007; Carlson et al. 2007, 2011). Here, we identify some of them as compact PMS sub-clusters that host objects at very early evolutionary stages, indicating their extreme youthfulness. Sub-cluster 2 is a characteristic example of a compact cluster at earlier stages of formation, since it is highly embedded (see, e.g., Carlson et al. 2007; Gouliermis et al. 2007), as opposed to sub-cluster 1, which appears to be clean from any nebula. Candidate YSOs are

found to coincide with two additional sub-clusters (9 and 12), for which the few faint PMS stars cannot give us a reasonable age estimation. The bright IR emission of these sub-clusters, as well as their few optically detected PMS members indicate that these are highly embedded clusters.

4.4. The Distribution of PMS stars within NGC 602

The main cluster of the region, NGC 602, is the dominant PMS stellar concentration. While NGC 602 is being classified as a single group, based on the 2σ isopleth in the stellar density map of Fig. 5, one can observe in the same map that there are multiple high density peaks within the boundaries of the cluster, suggesting that the cluster itself is a multiple stellar group. However, there are two observational biases, which can affect the two-dimensional spatial distribution of stars in a cluster, giving false evidence of multiple stellar density peaks. The first is extinction, which hides the fainter stars of the cluster with differential reddening within the cluster allowing only patches of a homogeneous stellar concentration to appear as density peaks. The second is confusion in the stellar photometry, which due to crowding or high sky contamination can produce an effect of multiplicity, since the inefficient detectability of stars at some parts of the cluster would produce the appearance of different peaks within the cluster. Concerning the first bias a maximum value for extinction of $A_V \simeq 0.3$ mag, based on our reddening measurements (Schmalzl et al. 2008) is not high enough to significantly hide portions of stars in the cluster. The low extinction of the cluster is further verified by the ancillary H α HST observations and from imaging with STT of the region (see, e.g., Figs. 1 and 2 respectively

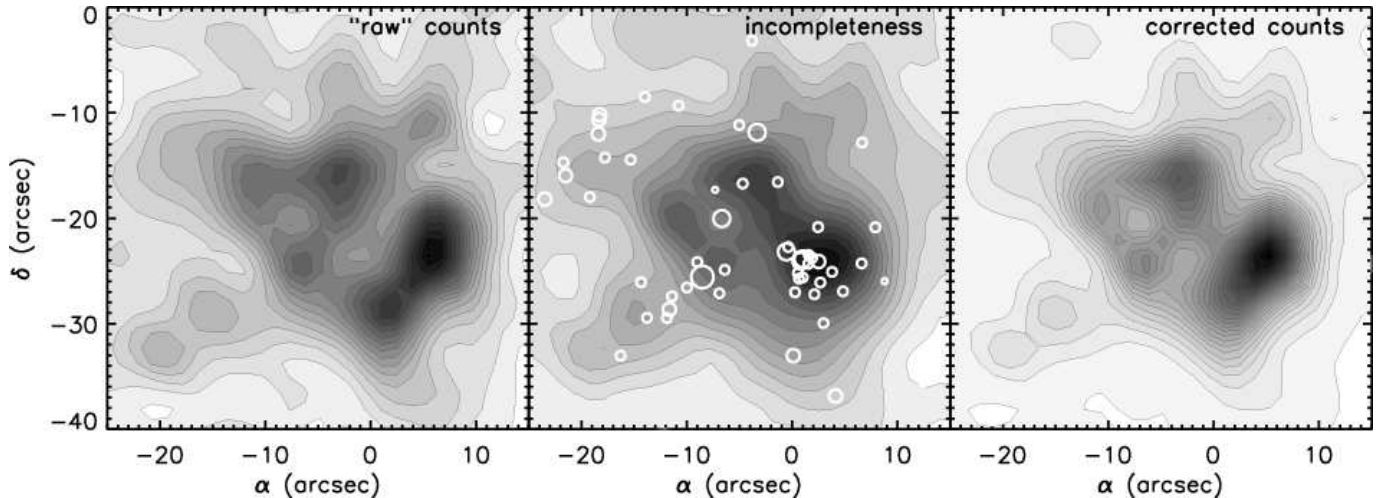


FIG. 9.— Isodensity contour map of the central cluster NGC 602. *Left*: The map constructed from ‘raw’ counts on the original observed numbers of low-mass PMS stars with no correction for incompleteness applied. *Middle*: The corresponding ‘completeness’ map, constructed by counting stars from our fake star experiments. Dark grey contours correspond to areas with the least success in recovering stars in the photometry, i.e., with the higher incompleteness. Light grey contours correspond to areas with the highest detecting efficiency, i.e., higher completeness in our photometry for low-mass PMS stars. Open white circles correspond to the UMS in the area of NGC 602. There is an apparent relation between incompleteness and high concentration of such stars, indicating that crowding affects our photometric detection efficiency. *Right*: Same as the map in the left panel, but corrected for incompleteness according to the measurements shown in the middle panel. This density map shows that sub-clustering within the boundaries of the cluster is not the result of incompleteness alone, but a real phenomenon. All maps are plotted at the same scale.

in Carlson et al. 2007). These observations show that the gas and dust content in the bubble of the region is quite low, being removed towards its edges and leaving the cluster quite clean from extinction.

On the other hand, confusion in the detection of stars, and therefore incompleteness in our photometry, may be a more important factor in the appearance of multiple density peaks in the cluster. We quantified the incompleteness in our photometry on the basis of artificial star experiments in Schmalzl et al. (2008). As a consequence, we are able to determine the completeness of our photometry not only as a function of magnitude and color, but also of position. In order to assess if indeed incompleteness is enough to explain the apparent multi-peaks in stellar density within NGC 602, we construct an *incompleteness map* of the area of the cluster, by applying the same star-counts technique to the artificial stars catalog with that we used for the construction of the stellar density map of Fig. 5. For reasons of comparison, we construct the incompleteness map with the same input parameters as for the stellar density map of the region (see § 4.1).

In Fig. 9 (left panel) we show the part of the stellar density map of Fig. 5 centered on NGC 602. In the middle panel of the figure is shown the incompleteness map for the same area. Darker grey tones correspond to higher incompleteness, i.e., lower detectability of stars. We overlay the positions of the most bright UMS stars in the area of the cluster to demonstrate that higher incompleteness is related to these stars, and thus indeed it is the product of confusion. We do not count stars with completeness less than 40% in both filters, as derived with our artificial star experiments in Schmalzl et al. (2008). We correct the original star-count map of the cluster according to the incompleteness map. From the completeness-corrected map, shown in the right panel of Fig. 9, it is seen that the south-western double density peak, at the right of the original map (left panel), has become a larger single peak. However, the appearance of different peaks within the cluster has not been eliminated, even after our correction for incompleteness. This gives evidence that the fragmented appearance of the cluster is real, and that photometric confusion can only

partly account for it.

4.5. The diffuse PMS population

The spatial distribution of low-mass PMS stars, shown in Fig. 5, demonstrates the existence of statistically significant distinct stellar concentrations, which we classify as compact PMS sub-clusters in the previous sections. However, the spatial distribution of low-mass PMS stars shows also that these sub-clusters are surrounded by a general diffuse distribution of the same kind of stars. This clearly indicates that while these sub-clusters are distinct stellar groups, they are not totally independent. They are possibly dynamically and even evolutionarily related to each other. The diffuse PMS population accounts for the $\sim 40\%$ of the total PMS population observed in the region, i.e., 60% of the total detected PMS stars are clustered. This fraction is higher than in the SMC star-forming region NGC 346/N66, where we found only about 40% of the PMS stars in clusters (Schmeja et al. 2009).

We consider as members of the diffuse population all PMS stars located at areas of stellar density less than 2σ , as indicated by the pink color in the density map of Fig. 5. This selection is based on the fact that the 2σ isopleth sets the boundaries of all detected sub-clusters. The field-subtracted CMD of the diffuse PMS stars is shown in Fig. 10 with a set of FRANEC PMS isochrones similar to that shown in Fig. 8 overlaid. This CMD includes about 500 faint PMS stars, the CMD-loci of which demonstrate the same broadening as in the CMDs of the clusters, and therefore any age determination from them would not be accurate. On the other hand the few bright PMS, located on the transition between PMS-MS seem to fit best the 5 Myr isochrone, which clearly indicates that these stars may be somewhat older than the members of the small compact PMS sub-clusters, having ages close to those of NGC 602.

5. MINIMUM SPANNING TREE AND THE \mathcal{Q} PARAMETER

In order to further quantify the clustering of low-mass PMS stars in the region NGC 602/N90, we apply a second method, which makes use of a minimum spanning tree (MST), defined

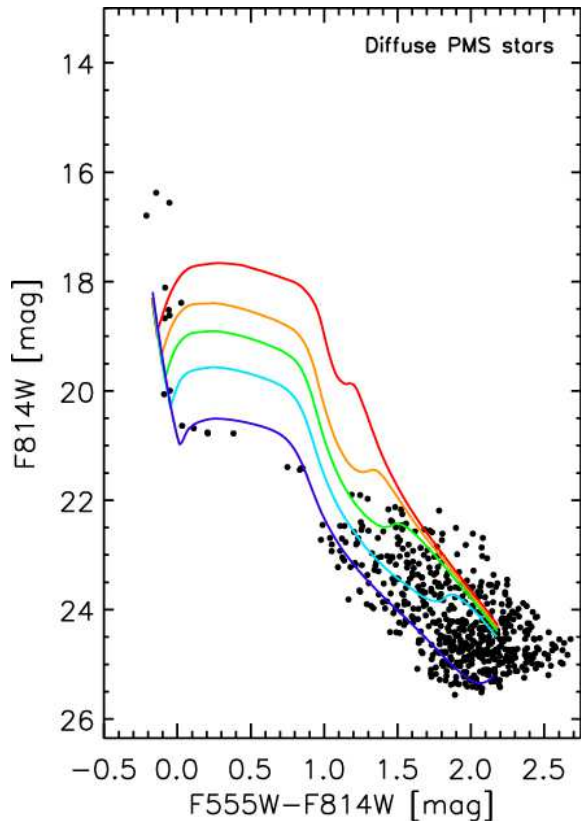


FIG. 10.— F555W–F814W, F814W CMD of the diffuse PMS stars in the region NGC 602/N90. PMS isochrone models calculated with `FRANEC` (Tognelli et al. 2011) are overlaid as in Fig. 8. They demonstrate that PMS stars not hosted by clusters possibly share the same formation history with those in NGC 602, being somewhat older than the members of the compact PMS sub-clusters.

as the unique set of straight lines (‘edges’) connecting a given set of points without closed loops, such that the sum of the edge lengths is a minimum (Borůvka 1926; Kruskal 1956; Prim 1957). In particular we make use of the Q parameter (Cartwright & Whitworth 2004), defined as $Q = \ell_{\text{MST}}/\bar{s}$, which combines the normalized correlation length \bar{s} , i.e. the mean distance between all stars, and the normalized mean edge length ℓ_{MST} derived by the MST for the cluster. It is a measure of the fractal dimension D of a stellar group, permitting us to quantify the structure of a cluster and to distinguish between clusters with a central density concentration and hierarchical clusters with possible fractal substructure. Large Q values ($Q > 0.8$) describe centrally condensed clusters having a volume density $n(r) \propto r^{-\beta}$, while small Q values ($Q < 0.8$) indicate clusters with fractal substructure. This method and the interpretation of Q , as developed by Cartwright & Whitworth (2004), is actually based on the three-dimensional structure of stellar systems. In particular, these authors constructed artificial three-dimensional clusters and studied the Q values for different two-dimensional projections to derive the correlation of Q with the radial density exponent β or the fractal dimension D . Q is correlated with β for $Q > 0.8$ and anticorrelated with D for $Q < 0.8$. Cartwright & Whitworth (2004) show that unlike centrally concentrated clusters, fractal clusters can look quite different in different projections, leading to a wider range in the Q parameter values. As a consequence, the three-dimensional structure affects more the fractal systems and this is the reason why the derived errors are larger for low Q values. A detailed description of the method, and in particular its implementa-

tion in this study, is given by Schmeja & Klessen (2006).

We assess the structural status of the PMS sub-clusters detected in the region NGC 602/N90 by applying the MST method on the samples of PMS stars of each sub-cluster. One important limitation to this application is the total number of points in each set. With decreasing number of objects, n , the error of Q increases, and the value becomes less meaningful. We made an estimation of the Q measuring accuracy with the use of artificial clusters, which we constructed with specific density profiles, and for which we computed the average Q and its standard deviation, σ_Q , from 100 different realizations. From our experiments we found a general degeneration of Q with decreasing n . For smaller n the value of Q for centrally concentrated clusters stays roughly constant and higher than 0.8. On the other hand, for fractal clusters with smaller n , Q rises toward and even over 0.8, providing false evidence that they are centrally concentrated.

This behavior was more apparent for artificial clusters with $\lesssim 30$ members. Therefore, while in Table 1 we give a Q value for all sub-clusters detected in NGC 602/N90, our analysis will be mainly based only to those with more than 30 members (where $\sigma_Q \lesssim 10\%$), i.e., for the five more populous sub-clusters. The derived Q values and typical uncertainties in their determination, derived from our artificial clusters experiments, are given in Cols. 9 and 10 of Table 1 respectively. From these values it can be seen that almost all considered clusters lie on the limit between being centrally concentrated and fractal. In particular NGC 602, which is quite populous and therefore its Q is more accurately determined, has the intermediate value of $Q = 0.8$. Among the sub-clusters with more than 30 members only one, sub-cluster 3, has a Q somewhat smaller but still very close to this threshold. About two-thirds of the poorer sub-clusters, i.e., those with less than 30 members, have Q values that classify them as centrally concentrated, or position them very close to the limit between centrally concentrated and fractal clusters. However, as mentioned above, this result is unreliable, because of the lower accuracy in the determination of the Q parameter of these clusters. It should be noted that all Q values are derived from the faint PMS stars alone, but the use of both PMS and UMS stars included in each sub-cluster delivers almost the same values, not altering at all our results, possibly because the number of additional sources is very low.

We assess the structural behavior of the diffuse PMS stars by considering the sample of all PMS stars, the density of which corresponds to the average stellar density in the region, as if the whole structure represents one stellar concentration. The reason for this treatment, which also considers all detected sub-clusters as part of the diffuse population, is that there would be no physical meaning to determine the behavior only of the PMS stars in the ‘inter-cluster’ area, since such a patchy stellar distribution is not real. This application of the MST method for the complete sample of PMS stars derives a Q value of 0.85, well above the threshold of 0.8 toward the Q values for centrally concentrated clusters. This result provides solid evidence that the whole agglomeration of PMS stars in the region can be itself treated as a centrally concentrated cluster as well (see also Fig. 11). However, if the UMS stars are considered also the value drops to $Q = 0.75$, due to the more ‘clumpy’ distribution of these stars. While this value is still not low enough to safely characterize the structure as fractal, it certainly suggests that this concentration is hierarchically structured. In any case, our results indicate that the diffuse PMS population is dynamically related, if not bound,

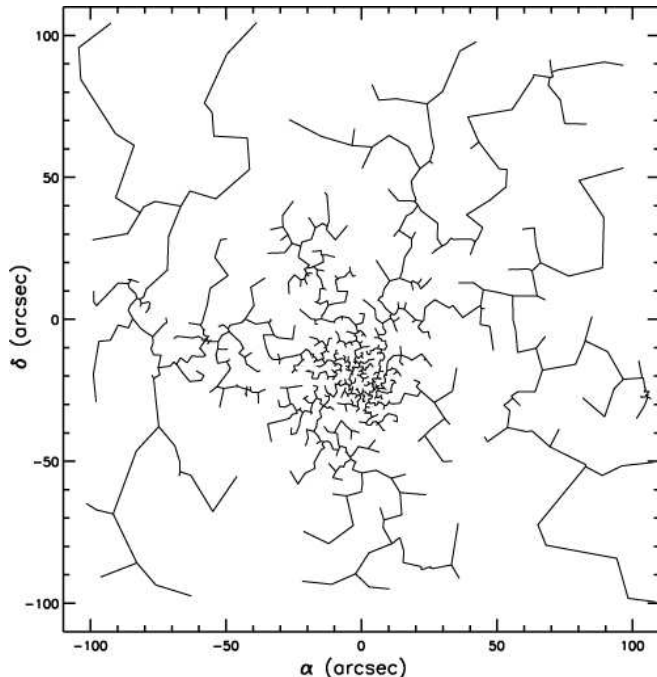


FIG. 11.— The MST graph for the entire low-mass PMS population observed in the region NGC 602/N90.

to the clustered population, and that the individual PMS sub-clusters themselves are tightly related to each other.

6. A SCENARIO OF CLUSTERED STAR FORMATION IN NGC 602/N90

Our results above on the clustering behavior of PMS stars, in conjunction to those on the age differences between the observed PMS populations in the individual sub-clusters and the inter-cluster area (§§ 4.3 and 4.5), leads us to the construction of a star cluster formation scenario in NGC 602/N90. According to this scenario PMS stars were formed $\lesssim 5$ Myr ago clustered at the center of the bubble, where NGC 602 is located, with a swift following formation of stars $\lesssim 2.5$ Myr ago in the peripheral small compact sub-clusters. It is worth noting that these timescales are consistent with those derived from the YSOs in the region by Carlson et al. (2011). This scenario is also in a very good agreement with the result by Nigra et al. (2008) that star formation in the region initiated ~ 4 Myr ago, and with the results by Cignoni et al. (2009), according to which the star formation rate in the region seems to have increased with time, with a peak at ~ 2.5 Myr ago. This short timescale between the two indicative stellar generations is in accordance to the paradigm of rapid star formation on dynamical time-scales (e.g., Elmegreen 2000; Hartmann 2001), as opposed to that of slow star formation (e.g., Shu et al. 1987).

The short timescale between the star formation events may also explain the origin of the diffuse PMS stars. Theoretical studies of early cluster dissolution, show that a timescale of few Myr is long enough for a cluster to start evaporating and feed the surrounding field with low-mass stars due to violent relaxation induced by the expulsion of its residual star-forming gas (e.g., Kroupa 2008; Parmentier 2010). This, considering the somewhat older age of the diffuse PMS population in the area between the sub-clusters, may track the origin of these stars back at the central cluster NGC 602, which started evaporating almost immediately after formation. Indeed, the MST graph of Fig. 11 for the whole de-

tected sample of PMS stars, shows that these stars appear to be distributed almost symmetrically around NGC 602, as if they originated there. In addition, theoretical studies suggest that cool, clumpy young clusters dynamically mass segregate on a short timescale, undergoing core collapse events, which can blow the clusters apart even with no need for gas expulsion (Allison et al. 2010). Such processes may take place in the compact sub-clusters, still in their natal gas, which then would also contribute to the diffuse low-mass PMS population. The same simulations showed that massive stars are often ejected from the cluster shortly after its formation with an average escape velocity of 2.5 km s^{-1} . It is interesting to note that this velocity is consistent with the upper limits for HI shell-expansion velocity from Nigra et al. (2008). If we consider the upper age limit of 5 Myr for NGC 602, this escape velocity would account for a distance of about 13 pc of a star from the cluster. Interestingly, this is almost identical to the projected radial distance, ~ 12 pc, of the most remote massive star, the O6 dwarf star #8 in Hutchings et al. (1991) catalog. It is worth noting that 50% of the hot massive stars in this catalog are located outside the boundaries of NGC 602, as they are defined by the 2σ isopleth in the density map of Fig. 5.

Based on the discussion above we conclude that the central part of the region NGC 602/N90 is experiencing a multi-system active star formation for the last $\lesssim 5$ Myr. The original event formed the cool, clumpy cluster NGC 602, which rapidly started dissolving into its immediate ambient, while becoming more compact at its center. Star formation continued taking place at the rim of the surrounding dusty nebular ring, in compact PMS sub-clusters, which are still half-embedded in their natal gas and bright in IR wavelengths. This process produced a diffuse inter-cluster PMS population originating from the clusters dissolution and introduced an age-spread among the various PMS populations of the order of 2.5 Myr.

7. CONCLUDING REMARKS

In this study we make use of the rich sample of PMS stars detected with ACS/WFC in the region NGC 602/N90 in the SMC to investigate the clustering behavior of these stars, and derive conclusions on the origin of this behavior. We apply star-counts of PMS stars and we identify 14 distinct sub-clusters in terms of their high surface density with respect to the average background stellar density in the region. The cluster NGC 602 is identified as the dominant stellar concentration in the region, located almost at the center of the ring-shaped nebula N90. This cluster's stellar distribution is spatially asymmetric. It is also found to be multi-peaked with few distinct stellar over-densities within its boundaries. We verify that this multiplicity is real, since variable extinction is not high enough to produce it, and photometric confusion can account for it only partly. We find that the spatial distribution of the PMS stars in the whole region is bimodal, with $\sim 60\%$ of the total PMS population being included in the sub-clusters, and the remaining forming a diffuse population distributed in the inter-cluster area, covering the whole central part of the nebula with a higher concentration towards east.

We construct the CMDs of the detected clusters from all stars encompassed in the 2σ isopleth in the stellar density maps that defines the boundaries of each sub-cluster. The age of young clusters cannot be determined directly from isochrone fitting of their low-mass PMS stars on the CMD. The reason is that observational and physical factors produce

a broadening of these stars in the CMD that confuses the fitting process. As a consequence any isochrone fitting derives unrealistic age spreads. On the other hand the positions of intermediate-mass PMS stars are less affected by these factors, and therefore they are better tracers of the age of the cluster. We were able to establish upper limits on ages from these stars only for the eight most populous sub-clusters, on the basis of isochrone fitting on the CMDs of the clusters, after the contamination by the background general field of the galaxy was statistically subtracted. We find that there is a noticeable difference in the age of NGC 602 from that of its surrounding compact sub-clusters, of the order of ~ 2.5 Myr. The somewhat younger age of the compact sub-clusters is further supported by their half-embedded status, which makes them bright in the IR, and some of them even coincide with candidate massive YSOs detected with SST. On the other hand, most of the gas in NGC 602 seems to be expelled, which attests to its more evolved nature. An age estimate similar to that for NGC 602 was found also for the diffuse PMS population from the corresponding CMD. Neither the clustered nor the diffuse PMS population is found to be older than ~ 5 Myr.

We apply the MST method and quantify the clustering behavior of PMS stars with the Q parameter. This application is not meaningful for clusters with less than 30 members, due to the derived uncertainties, and therefore our analysis focuses only on the five most populous sub-clusters. We find that almost all of them are centrally concentrated, with NGC 602 having $Q = 0.8$, on the limit separating centrally concentrated from possible fractal clusters. These results do not change when the UMS stars of the clusters are included in the Q determination also. Judging from the smaller sizes and higher densities of the poorer sub-clusters, as well as from their tentative Q values, we assess that they should be quite compact and not hierarchical. Considering the clustering behavior of the diffuse PMS population, we evaluate it from all detected PMS stars with surface density corresponding to the average stellar density in the region, and therefore also including the detected sub-clusters. We find that $Q = 0.85$ for the low-mass PMS stars and $Q = 0.75$ when also the UMS are included. These numbers do not allow a clear characterization of the stellar concentration as centrally concentrated or possibly fractal, but they show that the complete PMS stellar popu-

lation of the central area of NGC 602/N90, both clustered and diffuse, seem to behave as a coherent stellar concentration in terms of dynamical and stellar evolution.

Taking into account the fact that young star clusters start to evaporate rapidly due to the expulsion of their natal gas or due to early dynamical evolution, and based on the results discussed above we propose a scenario that may explain the cluster formation in the region NGC 602/N90. According to this scenario star formation took place in multiple high-density areas during a period of 2.5 Myr, less than 5 Myr ago. The clumpy cluster NGC 602 at the center of the nebula seems to have formed first, and possibly it started dissolving, sending low-mass PMS stars in its surrounding ambient, shortly after its formation. More recent star formation occurred in individual compact sub-clusters, which also may have fed the field with evaporating low-mass PMS stars. There are no indications if the two star formation events are actually sequential or not, but the small age spread of the infant PMS stars and their clustering behavior indicates that the whole central part of the region is dominated by a single loose stellar concentration, characterized by multiple high density peaks, which are bright in the IR and a central larger cluster which has most of its gas expelled. If the hot bright stars included in this system are considered then this stellar concentration may possibly classify as a stellar association in the making. However, the validity of this claim depends on the stability of the system, which needs to be further investigated through its dynamical behavior.

D.A.G. kindly acknowledges financial support by the German Aerospace Center (DLR) and the German Federal Ministry for Economics and Technology (BMWi) through grant 50 OR 0908. S.S. was supported by DFG through grants SCHM 2490/1-1, KL 1358/5-2 and SFB 881 “The Milky Way System”. This work is based on observations made with the NASA/ESA *Hubble Space Telescope*, obtained from the data archive at the Space Telescope Science Institute (STScI). STScI is operated by the Association of Universities for Research in Astronomy, Inc. under NASA contract NAS 5-26555.

REFERENCES

- Allison, R. J., Goodwin, S. P., Parker, R. J., Portegies Zwart, S. F., & de Grijs, R. 2010, *MNRAS*, 407, 1098
- Battinelli, P., & Demers, S. 1992, *AJ*, 104, 1458
- Borůvka, O. 1926, *Práce moravské přírodovědecké společnosti*, 3, 37
- Bourke, T. L., Myers, P. C., Robinson, G., & Hyland, A. R. 2001, *ApJ*, 554, 916
- Brott, I., & Hauschildt, P. H. 2005, *The Three-Dimensional Universe with Gaia*, 576, 565
- Bruck, M. T. 1976, *Occasional Reports of the Royal Observatory Edinburgh*, 1, 1
- Carlson, L. R., et al. 2007, *ApJ*, 665, L109
- Carlson, L. R., et al. 2011, *ApJ*, 730, 78
- Cartwright, A., & Whitworth, A. P. 2004, *MNRAS*, 348, 589
- Castelli, F., & Kurucz, R. L. 2003, *Modelling of Stellar Atmospheres*, 210, 20P
- Chieffi, A., & Straniero, O. 1989, *ApJS*, 71, 47
- Cignoni, M., et al. 2009, *AJ*, 137, 3668
- Clark, P. C., & Bonnell, I. A. 2005, *MNRAS*, 361, 2
- D’Antona, F., & Montalbán, J. 2003, *A&A*, 412, 213
- Da Rio, N., Gouliermis, D. A., & Gennaro, M. 2010, *ApJ*, 723, 166
- Degl’Innocenti, S., Prada Moroni, P. G., Marconi, M., & Ruoppo, A. 2008, *Ap&SS*, 316, 25
- Davies, R. D., Elliott, K. H., & Meaburn, J. 1976, *MmRAS*, 81, 89
- Dolphin, A. E. 2000, *PASP*, 112, 1383
- Elmegreen, B. G. 2000, *ApJ*, 530, 277
- Elmegreen, B. G. 2010, *IAU Symposium*, 266, 3
- Efremov, Y. N., & Elmegreen, B. G. 1998, *MNRAS*, 299, 588
- Elmegreen, B. G., & Scalo, J. 2004, *ARA&A*, 42, 211
- Gennaro, M., Prada Moroni, P. G., & Tognelli, E. 2011, *MNRAS* accepted (arXiv:1110.0852)
- Girardi, L., Bertelli, G., Bressan, A., Chiosi, C., Groenewegen, M. A. T., Marigo, P., Salasnich, B., & Weiss, A. 2002, *A&A*, 391, 195
- Goodman, A. A., Rosolowsky, E. W., Borkin, M. A., Foster, J. B., Halle, M., Kauffmann, J., & Pineda, J. E. 2009, *Nature*, 457, 63
- Gouliermis, D. A., Quanz, S. P., & Henning, T. 2007, *ApJ*, 665, 306
- Gouliermis, D. A., Chu, Y.-H., Henning, T., Brandner, W., Gruendl, R. A., Hennekemper, E., & Hormuth, F. 2008, *ApJ*, 688, 1050
- Gouliermis, D. A., et al. 2010, *The Impact of HST on European Astronomy*, 71
- Gouliermis, D. A., Dolphin, A. E., Robberto, M., et al. 2011, *ApJ*, 738, 137
- Hartmann, L. 2001, *AJ*, 121, 1030
- Henize, K. G. 1956, *ApJS*, 2, 315
- Hodge, P. 1985, *PASP*, 97, 530
- Hutchings, J. B., Cartledge, S., Pazder, J., & Thompson, I. B. 1991, *AJ*, 101, 933
- Jeffries, R. D. 2011, *Star Clusters in the Era of Large Surveys*, in press (arXiv:1102.4752)

- Kontizas, M., Kontizas, E., Dapergolas, A., Argyropoulos, S., & Bellas-Velidis, Y. 1994, *A&AS*, 107, 77
- Klessen, R. S., & Burkert, A. 2000, *ApJS*, 128, 287
- Kroupa, P. 2008, *The Cambridge N-Body Lectures*, 760, 181
- Kruskal, J. B. Jr. 1956, *Proc. Amer. Math. Soc.*, 7, 48
- Lada, C. J., & Lada, E. A. 2003, *ARA&A*, 41, 57
- Lee, H., Jackson, D. C., Skillman, E. D., Cannon, J. M., Gehrz, R. D., Polomski, E., & Woodward, C. E. 2005, *Bulletin of the American Astronomical Society*, 37, 1346
- Mac Low, M.-M., & Klessen, R. S. 2004, *Rev. Mod. Phys.*, 76, 125
- Massey, P., Waterhouse, E., & DeGioia-Eastwood, K. 2000, *AJ*, 119, 2214
- McKee, C. F., & Ostriker, E. C. 2007, *ARA&A*, 45, 565
- McLaughlin, D. E., and Pudritz, R. E. 1996, *ApJ*, 457, 578
- Nigra, L., Gallagher, J. S., III, Smith, L. J., Stanimirović, S., Nota, A., & Sabbi, E. 2008, *PASP*, 120, 972
- Parmentier, G. 2010, *IAU Symposium*, 266, 87
- Prim, R. C. 1957, *Bell Syst. Tech. J.*, 36, 1389
- Rolleston, W. R. J., Dufton, P. L., McErlean, N. D., & Venn, K. A. 1999, *A&A*, 348, 728
- Sabbi, E., et al. 2009, *ApJ*, 703, 721
- Schmalzl, M., Gouliermis, D. A., Dolphin, A. E., & Henning, T. 2008, *ApJ*, 681, 290
- Schmeja, S. 2011, *Astronomische Nachrichten*, 332, 172
- Schmeja, S., & Klessen, R. S. 2006, *A&A*, 449, 151
- Schmeja, S., Gouliermis, D. A., & Klessen, R. S. 2009, *ApJ*, 694, 367
- Sherry, W. H., Walter, F. M., & Wolk, S. J. 2004, *AJ*, 128, 2316
- Shu, F. H., Adams, F. C., & Lizano, S. 1987, *ARA&A*, 25, 23
- Simon, M., Dutrey, A., & Guilloteau, S. 2000, *ApJ*, 545, 1034
- Stahler, S. W., & Palla, F. 2005, *The Formation of Stars* (Weinheim: Wiley-VCH)
- Stanimirovic, S., Staveley-Smith, L., van der Hulst, J. M., Bontekoe, T. R., Kester, D. J. M., & Jones, P. A. 2000, *MNRAS*, 315, 791
- Stassun, K. G., Mathieu, R. D., Vaz, L. P. R., Stroud, N., & Vrba, F. J. 2004, *ApJS*, 151, 357
- Steffen, A. T., Mathieu, R. D., Lattanzi, M. G., et al. 2001, *AJ*, 122, 997
- Tognelli, E., Prada Moroni, P. G., & Degl'Innocenti, S. 2011, *A&A*, 533, A109
- Tognelli, E., Degl'Innocenti, S., & Prada Moroni, P. G., 2011b, in preparation
- Vallenari, A., Chiosi, E., & Sordo, R. 2010, *A&A*, 511, A79
- Ventura, P., Zeppieri, A., Mazzitelli, I., & D'Antona, F. 1998, *A&A*, 331, 1011
- Westerlund, B. E. 1964, *MNRAS*, 127, 429